

Conversion of RZ-OOK to RZ-BPSK by XPM in a Passive AlGaAs Waveguide

W. Astar, Paveen Apiratikul, Brice M. Cannon, Tanvir Mahmood, J. J. Wathen, John V. Hryniewicz, Subramaniam Kanakaraju, Christopher J. K. Richardson, T. E. Murphy, *Senior Member, IEEE*, and Gary M. Carter, *Fellow, IEEE*

Abstract—The conversion of data modulation format from 10-Gb/s return-to-zero on-off keying (RZ-OOK) to 10-Gb/s RZ binary phase-shift keying (RZ-BPSK) has been successfully carried out for the first time utilizing cross-phase modulation (XPM) in a passive AlGaAs waveguide. A 10^{-9} -bit-error-rate (BER) preamplified receiver sensitivity gain of ≈ 1 dB was measured for the converted RZ-BPSK relative to baseline RZ-OOK, whereas a penalty of ≈ 2.7 dB relative to baseline RZ-BPSK is explained to be due to cross-absorption modulation induced by nondegenerate two-photon absorption (ND-TPA), as well as to an insufficient nonlinear phase shift.

Index Terms—Cross-phase modulation (XPM), data modulation format conversion, nonlinear optics, two-photon absorption (TPA), waveguides.

I. INTRODUCTION

THE differential phase-shift keyed (DPSK) data format has attracted interest due to its theoretical 3-dB receiver sensitivity [or optical signal-to-noise ratio (OSNR)] advantage for balanced detection, relative to the conventional on-off keyed (OOK) data format, which doubles DPSK's propagation distance for transmission limited by amplified spontaneous emission [1]. Furthermore, it has been experimentally demonstrated that DPSK systems outperform OOK systems in dense wavelength-division-multiplexed transmission as the spectral efficiency exceeds 0.2 b/s/Hz because of its constant power

Manuscript received March 25, 2011; revised May 23, 2011; accepted June 08, 2011. Date of publication June 20, 2011; date of current version September 14, 2011.

W. Astar is with The Laboratory for Physical Sciences (LPS), College Park, MD 20740 USA and also with the Center for Advanced Studies in Photonic Research (CASPR), Baltimore, MD 21250 USA (e-mail: notilos@lps.umd.edu).

P. Apiratikul, J. J. Wathen, and C. J. K. Richardson are with The Laboratory for Physical Sciences (LPS), College Park, MD 20740 USA (e-mail: paveen@lps.umd.edu; WathenJJ@lps.umd.edu; Richardson@lps.umd.edu).

B. M. Cannon, T. Mahmood, and G. M. Carter are with The Laboratory for Physical Sciences (LPS), College Park, MD 20740 USA, and also with the Department of Computer Science and Electrical Engineering, University of Maryland, Baltimore County (UMBC), Baltimore, MD 21250 USA (e-mail: cannonb1@lps.umd.edu; Tanvir1@umbc.edu; carter@umbc.edu).

J. V. Hryniewicz was with The Laboratory for Physical Sciences (LPS), College Park, MD 20740 USA, and is now with Thorlabs Quantum Electronics Inc., Jessup, MD 20794-9608 USA.

S. Kanakaraju was with The Laboratory for Physical Sciences (LPS), College Park, MD 20740 USA, and is now with EpiWorks, Inc., Champaign, IL 61822-9598 USA.

T. E. Murphy is with the Department of Electrical and Computer Engineering, University of Maryland, College Park, MD 20742 USA (e-mail: TEM@umd.edu).

Color versions of one or more of the figures in this letter are available online at <http://ieeexplore.ieee.org>.

Digital Object Identifier 10.1109/LPT.2011.2160165

envelope, which mitigates the pattern-dependent XPM fiber impairment [2]. Because of the demonstrated advantages of DPSK systems, there have been some attempts at converting OOK to BPSK, in semiconductor optical amplifiers (SOAs) [3]–[5], and in nonlinear fiber [6]. Thus far, there have been no such experimental demonstrations in nonlinear, passive semiconductor waveguides. While SOAs can provide signal gain, they are relatively more complicated to fabricate, requiring multiple fabrication steps, current-injection control electronics, and efficient heat-sinking, whereas this is not the case with passive devices. The AlGaAs waveguide is a promising platform for nonlinear optical signal processing applications. In semiconductor waveguides such as silicon nanowires [7] and GaAs waveguides [8], nonlinear effects such as cross-phase modulation (XPM) and four-wave mixing (FWM) are degraded by two-photon absorption (TPA) and free-carrier effects induced by TPA. This problem can be significantly mitigated by using AlGaAs, whose bandgap energy can be engineered to minimize the effects of TPA throughout the telecommunication *C*-band. Moreover, the optical Kerr coefficient of AlGaAs is approximately 100 times larger than that of typical nonlinear fiber, and 4 times larger than that of *c*-Si [9]. This makes nonlinear optical signal processing possible in AlGaAs waveguides, obviating the need for submicrometer lithography. In this report, RZ-OOK-to-RZ-BPSK conversion by XPM in a passive AlGaAs waveguide is successfully demonstrated for the first time. We achieve a 10^{-9} -BER preamplified receiver sensitivity gain of ≈ 1 dB for converted RZ-BPSK relative to baseline RZ-OOK. Since the OOK signal is not precoded in the proposed scheme, a toggle flip-flop will be required to decode the data after direct-detection (not required for PRBS). However, decoding after detection will not be required for coherent reception.

II. EXPERIMENTS AND DISCUSSION

A. AlGaAs Waveguide Fabrication and Characterization

The device epistructure was grown using solid-source molecular beam epitaxy, on an *n*-GaAs substrate. It is comprised of three undoped layers: a 2.5- μm -thick $\text{Al}_{0.70}\text{Ga}_{0.30}\text{As}$ lower-cladding layer, a 0.5- μm -thick $\text{Al}_{0.23}\text{Ga}_{0.77}\text{As}$ guiding layer, and a 0.3- μm -thick $\text{Al}_{0.70}\text{Ga}_{0.30}\text{As}$ upper cladding. The peak photoluminescence wavelength of the guiding layer was 736 nm, designed to suppress two-photon absorption within the *C*-band. The waveguide was defined by projection lithography and inductively-coupled plasma etching. The etch depth was approximately 2.1 μm , creating deep-etched waveguides. The total device length was 10.8 mm, and consisted of 0.4-mm-long,

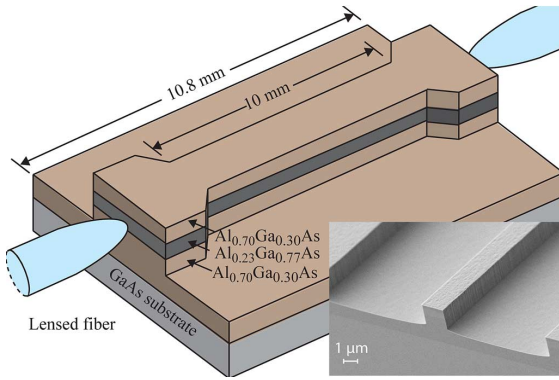


Fig. 1. Passive AlGaAs waveguide integrated with flared coupling structures to enable power exchange with lensed fibers. The scanning electron micrograph demonstrates a high-quality, anisotropic etch.

flared structures at the coupling planes to facilitate power exchange with lensed fibers (as shown in Fig. 1). The width of a flared structure was $3.5 \mu\text{m}$ at the coupling planes, and tapered to a fixed width of $1.5 \mu\text{m}$, which was the width of the 10-mm-long nonlinear waveguide. The device was characterized for propagation loss in accordance with the Fabry-Pérot method outlined in [10], and yielded losses of $\approx 2.7 \text{ dB}$ for the quasi-transverse-electric (QTE) mode, and $\approx 3.2 \text{ dB}$ for the quasi-transverse-magnetic (QTM) mode. The device was finally anti-reflection-coated with Si_3N_4 using plasma-enhanced chemical vapor deposition. The lensed fiber mode field diameter was $2.5 \mu\text{m}$. The total fiber-to-fiber device insertion loss was $\approx 13.2 \text{ dB}$ for the QTE mode, and $\approx 14.5 \text{ dB}$ for the QTM mode. After accounting for the measured propagation losses, the total coupling loss per facet (assuming identical coupling at both coupling planes) is estimated to be 5 dB for the QTE mode. The ensuing discussion addresses results for the lower loss polarization mode only.

B. Receiver Sensitivity Measurements

The experimental setup for the format conversion and receiver sensitivity measurement is shown in Fig. 2. The RZ-OOK pump signal was a 10 Gb/s (OC-192), 13%-duty-cycle, $2^{31} - 1$ PRBS at 1548 nm. The probe was a 10 GHz 9%-duty-cycle RZ clock signal at 1545 nm, generated using a commercially available (Oki) Franz-Keldysh-effect electroabsorption modulator (EAM), driven by an amplified clock signal recovered from the pump using a clock-recovery circuit. The duty cycles used were obtained by biasing the EAMs into deep absorption, and were the lowest allowed by the damage thresholds of the devices. The pump duty-cycle was larger than the probe duty-cycle in order to ensure a more uniform phase modulation over the duration of the probe pulse. The pump and probe were combined using a 90% fused-fiber coupler. After accounting for the input coupling loss, the respective pump and probe powers were $\approx 22 \text{ dBm}$ and $\approx 13 \text{ dBm}$. The polarization states of the pump and the probe were aligned by polarization controllers at the input of the coupler (Fig. 2). The probe was isolated by a bandpass filter (BPF) centered at 1545 nm at the output of the waveguide, which approximated the spectral profile of a flat-top, 100-GHz arrayed waveguide grating. The DPSK receiver consisted of a 4-dB-noise-figure, dual-stage preamplifier followed by 0.3-nm BPF, an asymmetric Mach-Zehnder interferometer (AMZI), a balanced



Fig. 2. RZ-OOK-to-RZ-BPSK format conversion setup.

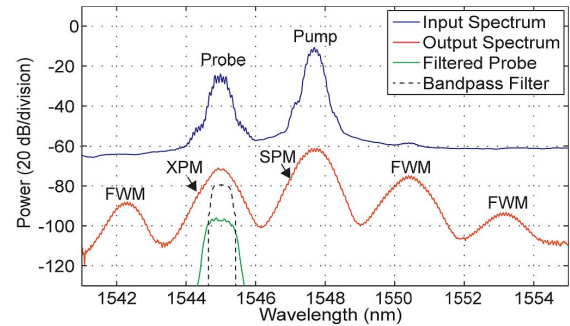


Fig. 3. Power spectra (optical spectrum analyzer (OSA) resolution bandwidth = 0.06 nm). The spectra have been offset for clarity. The output WDM trace also exhibits strong spectral broadening for the pump and the probe, and strong four-wave mixing (FWM) effects, with a (best) conversion efficiency greater than -5 dB .

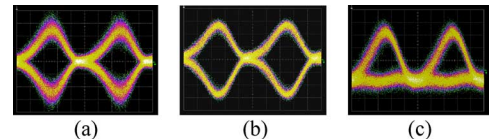


Fig. 4. The 50-GHz optical sampling module traces (20 ps/div.), displaying the output of a 12-GHz inverting transimpedance amplifier of the receiver, in infinite-persistence color-grade mode: (a) converted 10-Gb/s RZ-BPSK, (b) baseline 10-Gb/s RZ-BPSK, and (c) converted 10-Gb/s XAM. The OSNR was greater than 40 dB/0.1 nm for all traces. Trace (a) exhibits pattern-dependence compared to (b).

photodetector (BPD), an inverting transimpedance amplifier, clock recovery and a bit-error-ratio tester. A variable optical attenuator (VOA) was placed at the input of the preamplifier to vary the received power, and the corresponding OSNR was measured after the first stage of the preamplifier. Another VOA was located at the input of the BPD to maintain a consistent detected power for all of the measurements. For OOK receiver sensitivity measurements, the AMZI was bypassed and only the noninverting detector of the BPD was used.

The spectra at various locations in the experimental setup are shown in Fig. 3. The output WDM spectrum reveals significant spectral broadening in the pump and the probe. The OSNR of the probe at the output of the waveguide was greater than 40 dB/0.1 nm. The probe was observed to be fairly symmetric, showing little evidence of free-carrier effects.

Fig. 4(a) shows the probe, at the output of the waveguide and after the filter, and Fig. 5 shows the receiver sensitivity measurement results. Since receivers can respond differently to different signal duty-cycles [11], the RZ-OOK and RZ-BPSK signals used for the baseline measurements had the same duty-cycle (9%) as that of the converted RZ-BPSK signal, which was accomplished by launching RZ-OOK and RZ-BPSK into the same EAM used to generate the RZ clock. Fig. 5 shows that the converted RZ-BPSK signal (Fig. 4(a)), outperformed the baseline RZ-OOK signal by $\approx 1 \text{ dB}$ at 10^{-9} BER. Moreover, the baseline RZ-BPSK (Fig. 4(b)) signal outperforms the baseline RZ-OOK by $\approx 3.7 \text{ dB}$, while the converted RZ-BPSK signal suffers a penalty of $\approx 2.7 \text{ dB}$

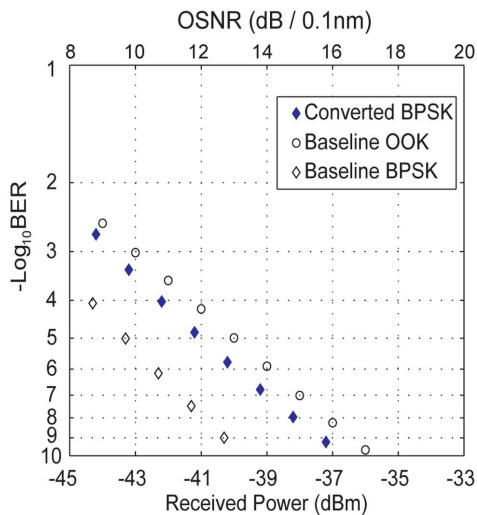


Fig. 5. Receiver sensitivity measurement results, demonstrating an approximate 1-dB receiver sensitivity gain for converted BPSK (solid blue diamonds) versus OOK (open circles).

compared to the baseline RZ-BPSK signal. A source of this penalty is thought to be due to residual pattern-dependent cross-absorption modulation (XAM) induced by ND-TPA. To confirm this, the RZ-clock modulation was turned off, resulting in a continuous-wave probe, and the receiver was configured to receive an OOK signal (as explained above), to which the probe output by the waveguide was directed. The detected signal is shown in Fig. 4(c), and demonstrates an RZ-OOK signal. The output probe directed at the DPSK receiver thus experienced simultaneous phase and amplitude modulation, the latter which contributed to the receiver sensitivity penalty. Theoretically, TPA should be negligible for pump/probe photon energies below half-the-bandgap energy of the guiding layer material, and we therefore ascribe the observed TPA to the two-photon equivalent of the Urbach tail, and some defect states [12]. The TPA coefficient was measured by the inverse transmission technique, and estimated to be 0.2 cm/GW, which is ≈ 50 times lower than that of GaAs [13] and 4 times lower than that of *c*-Si [9]. Another penalty source may have been an insufficient XPM phase shift, since in the conversion process, a mark in the RZ-OOK pump is supposed to result in a phase shift of π . The XPM phase shift of the probe was found to be $\approx 0.8\pi$ by estimating the spectral broadening of the pump pulses due to self-phase modulation (when only the pump was present in the waveguide). From theory {[14, fig. 4(b)]}, a 0.8π -phase-shift would be expected to yield a penalty of 1.7 dB – consequently, the majority of the 2.7-dB penalty is attributed to insufficient phase shift, while ≈ 1 dB is assigned to XAM-induced distortion.

The dispersion parameter at 1545 nm was measured [15] to be -0.9 ps/nm·m, and varied by 10%-maximum over the *C*-band. The computed pump-probe walk-off length of 17 cm was much longer than the physical length of the waveguide. Thus, pump-probe detuning over the *C*-band (35 nm) should result in no additional penalty.

III. SUMMARY AND CONCLUSION

The conversion of RZ-OOK-to-RZ-BPSK signals at 10 Gb/s in a passive AlGaAs waveguide has been successfully demon-

strated for the first time. A 10^{-9} -BER receiver sensitivity enhancement of ≈ 1 dB was found for converted RZ-BPSK signals compared to a baseline RZ-OOK signal, while a penalty of ≈ 2.7 dB was found relative to the baseline RZ-BPSK signal. The penalty was due to the presence of XAM (along with the requisite XPM) in the probe output by the waveguide, which led to amplitude modulation in the evaluated RZ-BPSK signal, and to an insufficient phase shift resulting from the large coupling loss. Further improvements of material and waveguide processing may lead to further mitigation of the ND-TPA, and to an enhancement of XPM.

REFERENCES

- [1] A. H. Gnauck and P. J. Winzer, "Optical phase-shift-keyed transmission," *J. Lightw. Technol.*, vol. 23, no. 1, pp. 115–131, Jan. 2005.
- [2] A. H. Gnauck, G. Raybon, S. Chandrasekhar, J. Leuthold, C. Doerr, L. Stulz, A. Agarwal, S. Banerjee, D. Grosz, S. Hunsche, A. Kung, A. Marhelyuk, D. Maywar, M. Movassaghi, X. Liu, C. Xu, X. Wei, and D. M. Gill, "2.5 Tb/s (64×42.7 Gb/s) transmission over 40×100 km NZDSF using RZ-DPSK format and all-Raman-amplified spans," in *Proc. OFC 2002*, Anaheim, CA, 2002, Postdeadline paper FC2.
- [3] W. Astar and G. M. Carter, "10 Gb/s RZ-OOK to BPSK format conversion by cross-phase modulation in SOA," *Electron. Lett.*, vol. 42, no. 25, pp. 1472–1574, Dec. 2006.
- [4] C. Yan, Y. Su, L. Yi, L. Leng, X. Tian, X. Yu, and Y. Tian, "All-optical format conversion from NRZ to BPSK using a single saturated SOA," *IEEE Photon. Technol. Lett.*, vol. 18, no. 22, pp. 2368–2370, Nov. 15, 2006.
- [5] H. Jiang, H. Wen, L. Han, and H. Zhang, "All-optical NRZ-OOK to BPSK format conversion in a an SOA-based nonlinear polarization switch," *IEEE Photon. Technol. Lett.*, vol. 19, no. 24, pp. 1985–1988, Dec. 15, 2007.
- [6] W. Astar, C.-C. Wei, Y.-J. Chen, J. Chen, and G. M. Carter, "Polarization-insensitive, 40 Gb/s wavelength and RZ-OOK-to-RZ-BPSK modulation format conversion by XPM in a highly nonlinear PCF," *Opt. Express*, vol. 16, no. 16, pp. 12039–12049, 2008.
- [7] W. Astar, J. B. Driscoll, X. Liu, J. I. Dadap, W. M. J. Green, Y. Vlasov, G. M. Carter, and R. M. Osgood, "All-optical format conversion of NRZ-OOK to RZ-OOK in a silicon nanowire utilizing either XPM or FWM and resulting in a receiver sensitivity gain of ~ 2.5 dB," *IEEE J. Sel. Topics Quantum Electron.*, vol. 16, no. 1, pp. 234–249, Jan./Feb. 2011.
- [8] W. Astar, P. Apiratikul, T. E. Murphy, and G. M. Carter, "Wavelength conversion of 10-Gb/s RZ-OOK using filtered XPM in a passive GaAs–AlGaAs waveguide," *IEEE Photon. Technol. Lett.*, vol. 22, no. 9, pp. 637–639, May 1, 2010.
- [9] M. Dinu, F. Quochi, and H. Garcia, "Third-order nonlinearities in silicon at telecom wavelengths," *Appl. Phys. Lett.*, vol. 82, no. 18, pp. 2955–2957, May 2003.
- [10] E. Kapon and R. Bhat, "Low-loss single-mode GaAs/AlGaAs optical waveguides grown by organometallic vapor phase epitaxy," *Appl. Phys. Lett.*, vol. 50, pp. 1627–1630, 1987.
- [11] P. J. Winzer and A. Kalmár, "Sensitivity enhancement of optical receivers by impulsive coding," *J. Lightw. Technol.*, vol. 17, no. 2, pp. 171–178, Feb. 1999.
- [12] D. C. Hutchings and E. W. V. Stryland, "Nondegenerate two-photon absorption in zinc blende semiconductors," *J. Opt. Soc. Amer. B*, vol. 9, pp. 2065–2074, 1992.
- [13] J. U. Kang, A. Villeneuve, M. Sheik-Bahae, G. I. Stegeman, K. Al-Hemyai, J. S. Aitchison, and C. Ironside, "Limitation due to three-photon absorption on the useful spectral range for nonlinear optics in AlGaAs below half band gap," *Appl. Phys. Lett.*, vol. 65, no. 2, pp. 146–148, Jul. 1994.
- [14] C.-C. Wei, W. Astar, J. Chen, Y.-J. Chen, and G. M. Carter, "Theoretical investigation of polarization-insensitive data format conversion of RZ-OOK to RZ-BPSK in a nonlinear birefringent fiber," *Opt. Express*, vol. 17, no. 6, pp. 4306–4308, 2009.
- [15] P. Merrit, R. P. Tatam, and D. A. Jackson, "Interferometric chromatic dispersion measurements on short lengths of monomode optical fiber," *J. Lightw. Technol.*, vol. 7, no. 4, pp. 703–716, Apr. 1989.